

Optical Measurement of a Compressible Shear Layer Using a Laser-Induced Air Breakdown Beacon

R. Mark Rennie¹, Garnett Cross.²
Center for Flow Physics and Control
University of Notre Dame, Notre Dame, IN, 46556

David Goorskey³, Matthew R. Whiteley⁴
MZA Associates Corporation, Dayton, OH, 45459

David Cavaleri⁵, and Eric J. Jumper⁶
Center for Flow Physics and Control
University of Notre Dame, Notre Dame, IN, 46556

The aero-optic aberrations due to a compressible shear-layer flow with high- and low-speed Mach numbers of 0.75 and 0.12 were measured using the return light from an artificial guide star. The guide star was created by focusing a pulsed, frequency-tripled Nd:YAG laser emitting in the ultraviolet to create a laser-induced air breakdown spark. The experiments showed that accurate wavefront data could be obtained, including accurate measurements of the wavefront tip/tilt, when the shear layer was forced and the measurements were phase-locked to the forcing signal. Issues involved in integrating the beacon system into a feedforward adaptive-optic correction approach are discussed.

Nomenclature

| | | |
|-----------------|---|--|
| D | = | turret diameter |
| D_{AP} | = | diameter of outgoing beam aperture |
| D_C | = | aperture of spark-collimating lens |
| D_L | = | beam diameter at focusing lens |
| f_C | = | focal length of spark-collimating lens |
| f_L | = | focal length of laser-focusing lens |
| M | = | Mach number |
| OPD | = | optical path difference |
| r | = | shear layer velocity ratio, U_1/U_2 |
| St | = | Strehl ratio |
| s | = | shear layer density ratio, ρ_1/ρ_2 |
| U | = | streamwise velocity |
| x | = | streamwise coordinate |
| δ_ω | = | shear-layer vorticity thickness |
| ε | = | spark "jitter" amplitude |
| Λ | = | shear-layer structure wavelength |
| λ | = | wavelength |
| ρ | = | density |

¹Research Assistant Professor, Department of Aerospace and Mechanical Engineering, Senior Member AIAA.

²Graduate Research Assistant, Department of Aerospace and Mechanical Engineering, Student Member AIAA.

³Scientist, MZA Dayton Operations.

⁴Vice-President, Senior Scientist, MZA Dayton Operations, Member AIAA.

⁵Research Specialist, Department of Aerospace and Mechanical Engineering, Member AIAA.

⁶Professor, Department of Aerospace and Mechanical Engineering, Fellow AIAA.

Subscripts

- 1 = low-speed flow
- 2 = high-speed flow

I. Introduction

ARTIFICIAL guide stars are under investigation as light sources for the measurement of nearfield flow-induced, or “aero-optic,” aberrations around aircraft traveling at compressible flight speeds [1, 2]. These artificial guide stars offer advantages over other options, such as natural light sources or glint from the target, due to the greater control over the location and timing with which they are generated. Measurement of aero-optic aberrations is an important component of possible adaptive-optic (AO) correction strategies [3]; even for feedforward AO approaches, in which the aero-optic aberrations are made more predictable using flow-control techniques, optical measurements are still necessary in order to synchronize the phase of the AO system with the phase of the flow-controlled aero-optic aberrations [4, 5].

One method of generating an artificial guide star is by focusing a high-energy pulsed laser at a point outside the aircraft, thereby creating an air-breakdown spark with brightness sufficient for optical measurements. In [1], an experimental investigation is described in which the aero-optic aberrations due to a compressible shear layer were measured using an artificial guide star that was simulated using the diverging light from an optical fiber. These results showed that anisoplanatism effects that originated from the fact that the guide star was a point source and illuminated only a small portion of the flow could be compensated [6] to produce an accurate estimation of the aberrations that would exist on a larger-aperture, planar-wavefront beam of light. In [2], experimental data are presented showing the optical quality of the return light from a laser-induced breakdown spark; these data showed that apparent jitter of the spark location results in “noise” on the wavefronts of the light from the spark, but that this wavefront noise would not affect the measurement of typical aero-optic flows if the optical system were carefully designed. This paper presents experimentally-measured wavefronts of a compressible shear-layer acquired using the return light from a laser-induced breakdown spark. For these experiments, the shear layer was forced and regularized, and the optical measurements were phase-lock-averaged to the forcing signal as a method of compensating for noise generated by the apparent spark jitter. Finally, issues associated with incorporating the spark into a feedforward AO correction approach for the shear-layer aberrations are discussed.

II. Experimental Approach

The problem under investigation is depicted in Fig. 1. The figure shows the flow past a hemispherical optical turret with a cylindrical base. A shear layer originates from the turret surface that is associated with the separated-flow region at the rear of the turret; at compressible flow speeds this shear layer becomes optically active such that the beam from the optical turret is severely aberrated when directed at targets in the aft field of regard. As the first step towards an AO correction, the aberrations due to the shear layer are measured using the return light from a laser-induced breakdown beacon. The beacon could be projected to any location in the vicinity of the turret that is suitable for illuminating the shear layer, including a point within the outgoing beam itself. Similarly, the aperture used to collect the return light from the beacon could be, for example, a side aperture mounted to the optical turret, or it could be the same aperture as used by the main beam.

The objective of the experiments was to evaluate the accuracy with which the aberrations of a realistic optically-active shear-layer flow could be measured

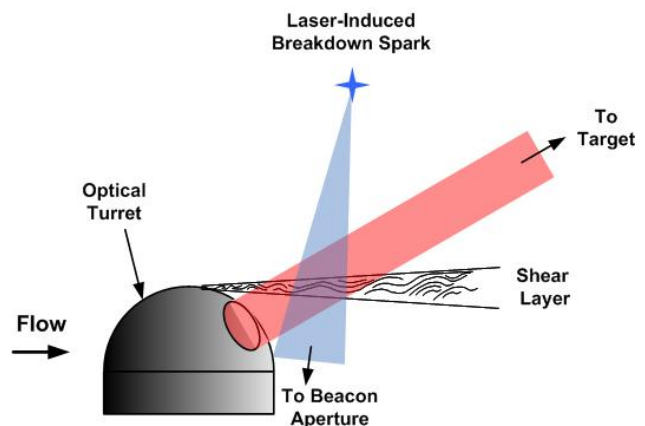


Fig. 1 Conceptual deployment of a laser-spark beacon system.

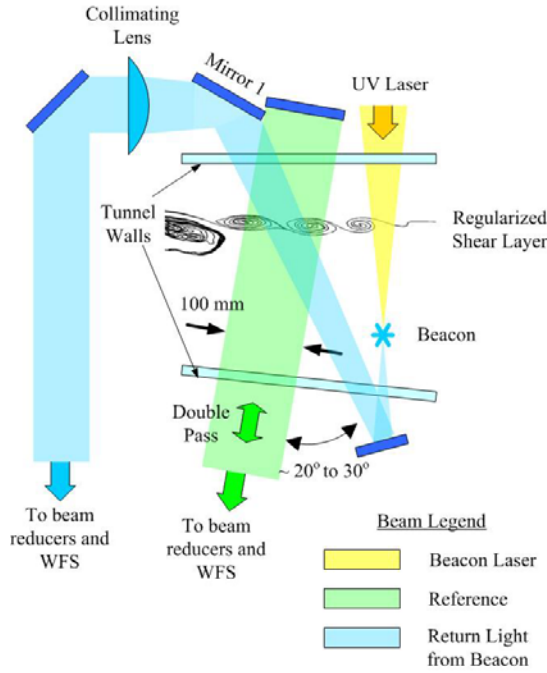


Fig. 2 Optical setup for wavefront measurements in Notre Dame Compressible Shear-Layer Wind Tunnel. The figure shows schematically the return light path from the beacon; Mirror 1 was actually aligned to direct the beacon light “out of the page.”

wavefront distortions act as “noise” on the spark wavefronts, that limit the ability of the beacon system to detect aero-optic aberrations that have an amplitude below the noise level. Figure 3 shows how the baseline noise of the beacon system depends on the optical system design; the red line in the figure shows the level at which the beacon wavefront noise would obscure aero-optic aberrations that would lower the Strehl ratio, Eq. (1), of a nominal $\lambda=1\mu\text{m}$ beam to 90% of its diffraction-limited performance:

$$St = \exp\left[-\left(\frac{2\pi \text{OPD}_{\text{rms}}}{\lambda}\right)^2\right] \quad (1)$$

Based on the data in Fig. 3, the lens used to focus the UV laser to generate the beacon had a focal length $f_L=300$ mm apertured to $D_L=20$ mm, giving a ratio $f_L/D_L=15$. The lens used to collimate the spark light had a focal length of $f_C=1200$ mm, and an aperture of $D_C=70$ mm giving $f_C/D_C=17$; as shown by Fig. 3, these f-numbers, $f_L/D_L=15$ and $f_C/D_C=17$, give acceptably-low levels of baseline noise on the spark wavefronts. With this optical system, the diameter of the diverging spark beam at the shear layer was approximately 50 mm, giving around 50% anisoplanatism with the 100 mm diameter reference beam, in addition to other anisoplanatism effects originating from the spherical curvature of the spark wavefronts and the approximately 25° misalignment of the spark and reference beams. A photograph of the optical setup in the CSLWT is shown in Fig. 4.

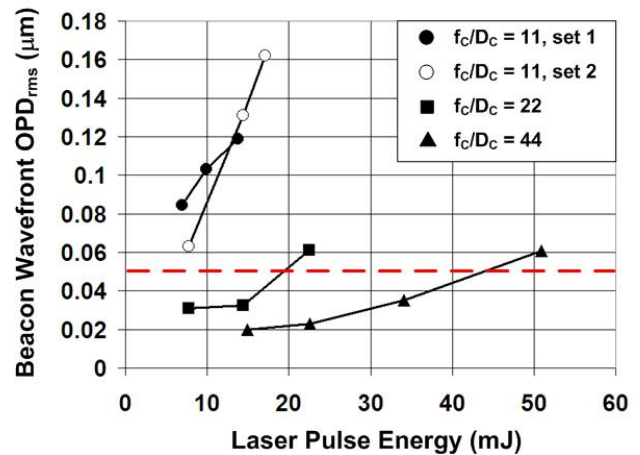


Fig. 3 Dependence of baseline spark wavefront noise on optical system parameters for $f_L/D_L=15$ [2]. Values below the dashed line correspond to $St>0.9$ for $\lambda = 1 \mu\text{m}$ radiation.

using a laser breakdown beacon as depicted in Fig. 1. The tests were conducted in the University of Notre Dame’s Compressible Shear-Layer Wind Tunnel (CSLWT), which mixes high- and low-speed flows with the same total temperature to produce the kind of full-scale compressible shear layer that would occur in the separated-flow region behind an optical mount such as a hemispherical turret [7, 8]. The shear-layer can also be regularized by applying mechanical forcing at the trailing-edge of the splitter plate that separates the high- and low-speed streams at the inlet to the CSLWT test section [4, 9]. Regularization of the shear layer in this way is used for investigation of feedforward AO approaches, or for synchronization of measurements with specific phases of the shear-layer aberration. The high- and low-speed Mach numbers used in the tests were nominally $M_2=0.75$ and $M_1=0.12$.

A schematic of the experimental setup is shown in Fig. 2. The reference beam was generated using a pulsed YAG laser emitting at 514 nm that had pulse durations that were sufficiently short to “freeze” the flow. The spark was formed by focusing a UV laser beam with $\lambda=355$ nm, after which the return light from the resulting breakdown spark was passed through the shear layer and collected using a collimating lens. As shown in [2], spark-to-spark motion of the effective location of the beacon produces distortions in the spark wavefronts; these

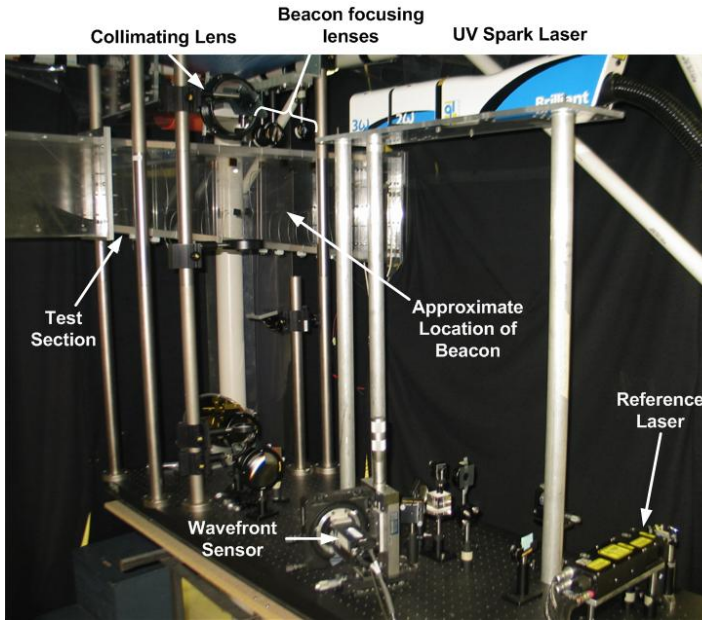


Fig. 4 Photograph of optical setup and wind-tunnel test section.

($0^\circ, 30^\circ, \dots, 330^\circ$) with respect to the period of the forcing signal. The phase-lock-averaged wavefronts from the reference and spark beams at each phase, with tip/tilt removed, are shown in Fig. 5; the figure clearly shows the progression of a sinusoidal-like aberration through the measurement aperture as the phase of the measurement changes. Figure 5 shows that the aberrations measured by the spark closely match those of the reference beam; a

As shown in Fig. 2, the UV laser beam was focused through the shear layer to create the air-breakdown beacon. This experimental arrangement simulates a possible operational deployment in which the beacon laser might be projected from the same aperture as the main beam, or from a nearby side-mounted aperture, so that it would project through the same shear layer as the main beam prior to spark formation.

A. Tip/Tilt-Removed Wavefronts

After passing through the shear layer, the return light from the beacon and the collimated reference beams were aligned side-by-side and projected into a single wavefront sensor that captured the wavefronts of both beams simultaneously. For these measurements, the shear layer was forced [4, 9] and the wavefront measurements were phase-locked to the shear-layer forcing with measurements made at 12 different phases

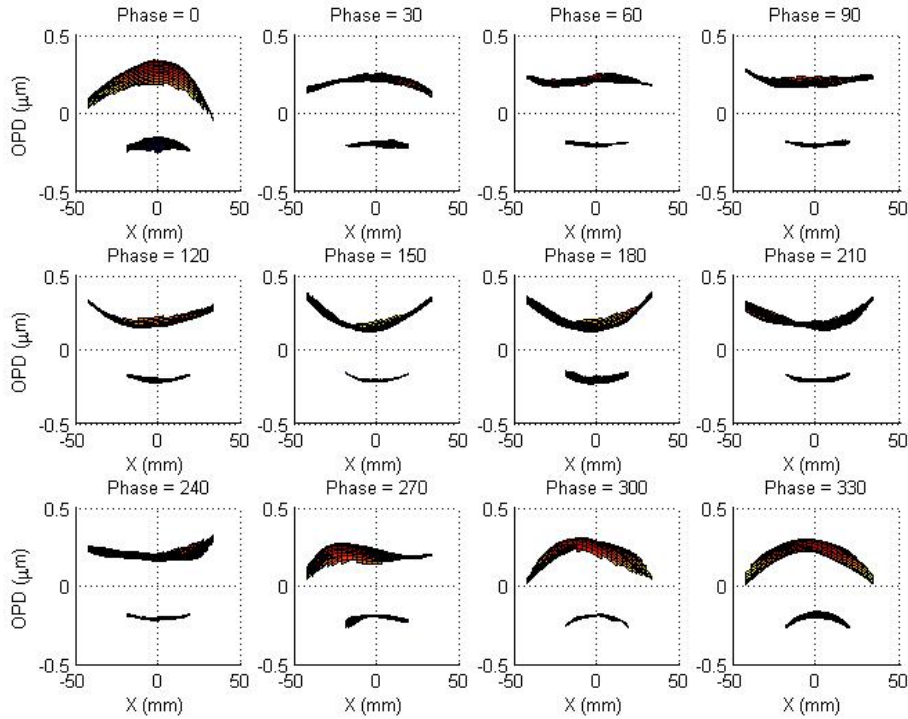


Fig. 5 Phase-lock-averaged wavefronts with tip/tilt removed acquired through forced shear layer. Reference beam is shown on top, spark beam shown on bottom of image for each phase.

statistical cross-correlation of the beacon and reference-beam wavefronts resulted in correlation coefficients in the range of 0.5 to 0.9.

B. Measurement of Streamwise Tilt

Figure 5 shows the phase-lock averaged aberrations with tip/tilt removed. As will be discussed later, it is helpful to retain the streamwise tilt information if the beacon is to be used for feedforward adaptive-optic corrections in the CSLWT; this tilt information is corrupted, however, by the same jitter in the effective location of the spark that produces the baseline aberrations shown in Fig. 3. The mechanism of the tip/tilt error is shown in Fig. 6, where ϵ is the amplitude of the effective spark motion. Figure 6 shows that the tip/tilt error is directly related to the effective lateral displacement of the origin of the light from the spark away from the optical axis of the collimating lens. Experimentally-measured streamwise “tilts” for a typical run using the setup shown in Fig. 2 are shown in Fig. 7, and confirm the model of Fig. 6.

Despite the large tip/tilt “noise” imposed on any single wavefront measurement by the spark jitter, Fig. 7 shows that this tip/tilt noise is random, so that accurate measurements of the tip/tilt of the forced shear-layer aberrations can still be obtained by phase-lock averaging. Figure 8 shows the same data from Fig. 5, this time with tip/tilt retained, and shows that the phase-lock-averaged wavefronts measured by the spark still closely match the wavefronts measured by the reference beam even with tip/tilt retained. One anomaly with the data in Fig. 8 is that there is a noticeable difference in the tilt of the wavefronts at 0° and 330° phase, so that it does not appear that the wavefront of the aberration would transition smoothly from the wavefront at 330° back into the wavefront at 0° phase; this discrepancy was likely caused by a small movement of the optical system over the 30 minute duration of the measurements, which added an additional tilt offset between the 0° and 330° phase measurements. Despite this discrepancy, the good agreement between the spark and reference wavefronts in Fig. 8 indicates that tip/tilt noise from the spark jitter can be “averaged out” by the phase-lock averaging process, so that the spark can still be used to accurately measure tip/tilt of the shear-layer aberration. It should be noted that the need for phase-lock averaging does not present an obstacle to an AO correction using a feedforward approach due to the long-term coherence and repeatability of the forced shear-layer aberrations.

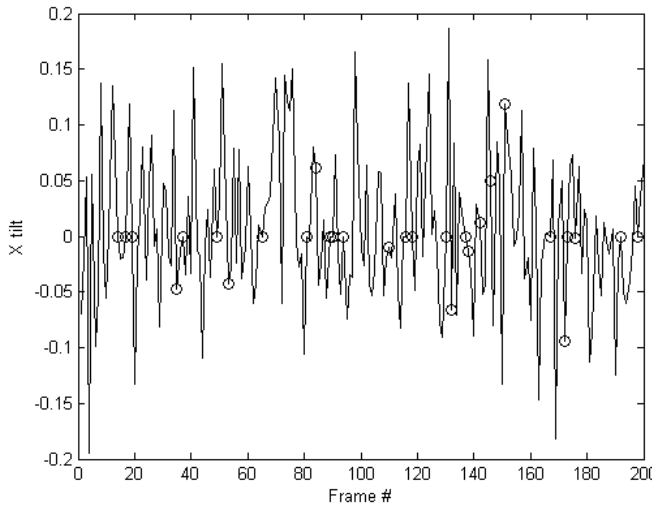


Fig. 7 Typical variation of streamwise tilt of spark wavefront due to apparent spark jitter. Tilt is shown in mrad.

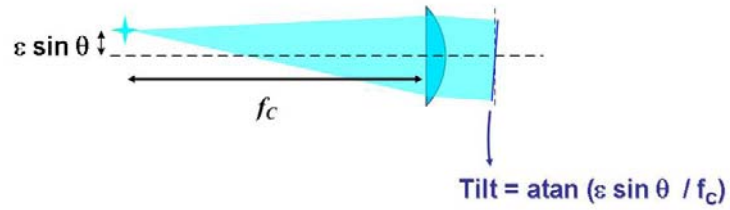


Fig. 6 Tilt cause by spark jitter. θ = angle between optical axis of lens and optical axis of UV laser beam.

III. Feedforward Adaptive-Optic Correction

One of the main motivations for developing an optical beacon system is to facilitate adaptive-optic correction of aero-optic flows. Particular emphasis is placed on the correction of compressible shear layer flows since this flow dominates, for example, the separated-flow region at the rear of optical turrets. As shown in [4, 5], one of the more promising correction methods is the feedforward AO approach, in which the shear layer is first regularized by controlled forcing applied at the point of origin of the shear layer. With the shear layer regularized, the deformable mirror (DM) is then pre-programmed with a shape that is the conjugate of the regularized shear-layer aberrations, after which the phase of the DM motion must be matched to the phase of the shear layer. Reference [4] describes a feedforward AO correction of this type in which the phase matching of the DM with the shear-layer aberrations was

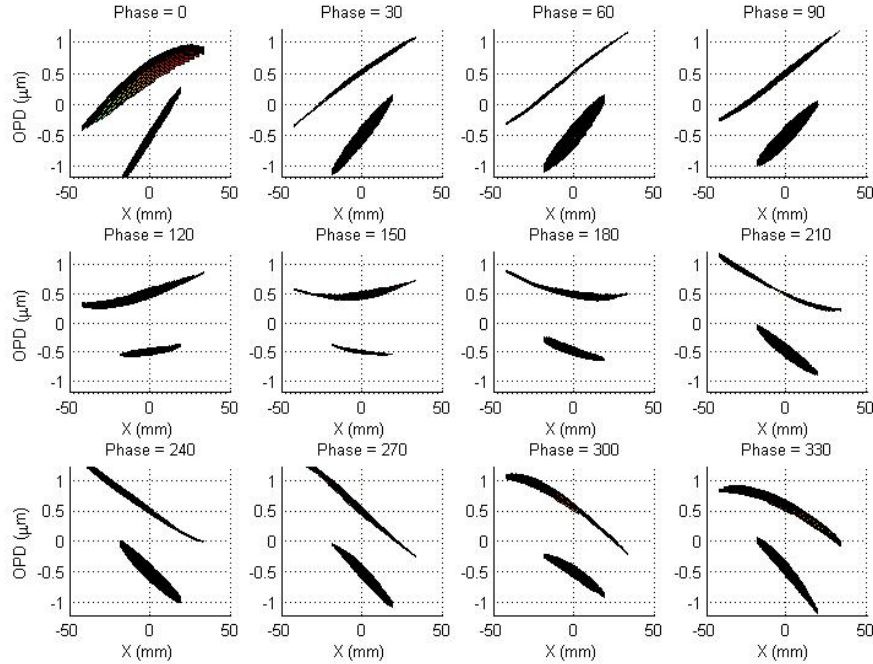


Fig. 8 Wavefronts from Fig. 5 with tip/tilt retained, showing that tip/tilt noise due to spark jitter can be compensated by phase-lock averaging of the optical data.

performed by a human operator who observed the corrected beam reflected from the DM. In reality, however, it would not be possible to observe the outgoing, corrected laser beam in this way; rather, for a realistic system, the phase and amplitude of the regularized shear layer would need to be measured using, for example, the return light from an artificial guide star such as described in this paper.

The advantage of the feedforward AO approach is that it is not necessary for the AO system to react to random, high-frequency aberrations associated with the un-regularized shear layer that are beyond the bandwidth capabilities of conventional feedback-type AO systems. Instead, for the feedforward approach, it is only necessary to initially adjust the phase and amplitude of the DM to match the regularized aberration and to periodically update these parameters to correct for any long-term flow fluctuations. As shown in [4], the update rate required to achieve a high quality correction is sufficiently slow that it can be adequately performed by a human operator. This slow update rate greatly alleviates the frequency requirements for both the AO and beacon systems.

A. Operational System

A schematic showing a possible layout for a realistic operational deployment of a laser-spark beacon system is shown in Fig. 9. The figure shows a hemispherical turret with cylindrical base with an optical aperture that is 1/3 the diameter of the turret ($D_{AP} = D/3$). As discussed above, good-quality wavefront measurements can be obtained using the return light from the laser spark if f_L/D_L and f_C/D_C both have the value of approximately 15 [2]. If the aperture of the spark and collecting lenses, D_L and D_C respectively, are approximately the same size as the turret aperture, then this means that $f_L \approx f_C \approx 15D_{AP} = 5D$, so that the beacon could be placed up to 5 turret diameters away from the turret. This situation is illustrated in

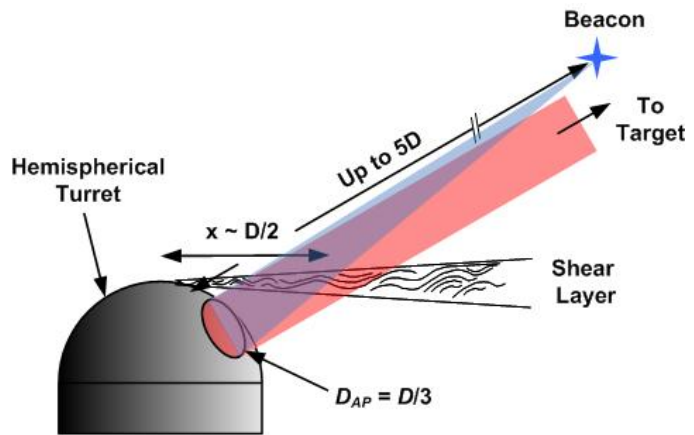


Fig. 9 Possible beacon geometry for a deployed system.

Fig. 9, which shows that the diameter of the return light cone from the beacon is almost the same diameter as the outgoing beam at the location of the shear layer.

If the shear layer is assumed to originate from the top of the turret, then for a nominal lookback angle of 45° past the vertical direction, the outgoing beam traverses the shear layer at a location $x \approx D/2$ downstream of the shear-layer origin. As shown in [10], the vorticity thickness δ_ω of the shear layer grows with distance x approximately as:

$$\delta_\omega/x = 0.085 \frac{(1-r)(1+s^{0.5})}{1+rs^{0.5}} \quad (2)$$

Setting the velocity ratio $r \approx 0.167$ for a typical shear-layer flow, and using $M_2=0.8$ as the cruise speed of a combat or transport aircraft, Eq. (2) gives $\delta_\omega/x \approx 0.125$. Furthermore, the shear-layer vorticity thickness δ_ω is approximately one-half of the structure wavelength Λ , so that $\Lambda/x \approx 0.25$. Finally, using $x \approx D/2 \approx 1.5 D_{AP}$ from Fig. 9, the shear-layer structure wavelength is approximately:

$$\Lambda \approx D_{AP}/3 \quad (3)$$

Equation (3) therefore shows that the outgoing beam for a typical optical turret spans on the order of 3 wavelengths of the dominant shear-layer disturbance. Note that, even if the shear layer were forced, the wavelength of the shear-layer disturbances would still be roughly equal to the values determined above using Eqs. (2) and (3). Since the return light from the beacon is nearly the same diameter at the shear layer as the outgoing beam (Fig. 9), then the beacon system would also capture approximately 3 wavelengths of the shear-layer aberration. With 3 wavelengths of the shear-layer aberration captured by the beacon, the phase of the shear-layer aberrations could be determined from the beacon wavefronts without the need to retain the tip/tilt information on the beacon wavefronts. As such, any tip/tilt noise on the beacon wavefronts due to the apparent jitter of the spark, as shown in Fig. 7, would have no effect on the performance of the beacon system since tip/tilt information would not be required in order for the beacon system to fulfill its function of determining the phase and amplitude of the shear-layer aberration. In particular, phase-lock averaging of the beacon wavefronts, as described above, would not be necessary to “average out” the tip/tilt noise; rather, the tip/tilt of the beacon wavefronts would simply be removed and the phase of the shear layer could be determined immediately from a single measurement.

Regularization of the shear layer also alleviates requirements on the design of the beacon optical system. In particular, with the shear layer regularized, the optical aberrations of the shear layer take the form of a repeatable waveform with frequency content primarily at the fundamental and subharmonic of the applied forcing frequency [4]; it is the conjugate of this waveform that is applied to the DM. As discussed above, when used in a feedforward AO application, the principal function of the beacon system is to measure the phase and amplitude of this dominant shear-layer aberration, which typically has an amplitude on the order of $0.6 \mu\text{m}$ or more [4]. Although further investigation is required, it is likely that acceptably accurate phase and amplitude measurements of the regularized shear-layer waveform could still be made if the beacon system had significantly higher noise levels than the $OPD_{rms} = 0.05$ limit shown in Fig. 3.

B. Wind-Tunnel Experiments

Feedforward AO correction tests will be performed in the near future in the CSLWT at the University of Notre Dame. The general optical setup for the tests will be very similar to that shown in Fig. 2. The shear layer will be forced using a signal with two frequency components consisting of a fundamental frequency of 750 Hz plus the first subharmonic; as shown in [4], this forcing produces the optimum regularization of the shear layer, with an aberration wavelength Λ on the order of 0.2 m. Due to practical limits on the sizes of the optical components, and due to the limiting constraints of the wind-tunnel walls, it will not likely be possible to capture a full wavelength of the shear-layer

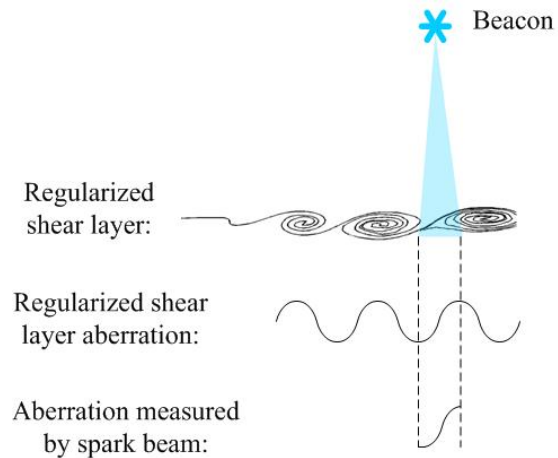


Fig. 10 Sketch showing effect of aperture on measurement of regularized shear-layer aberration.

aberration with the return light from the beacon. Instead, the beacon system will measure only a fraction of the wavelength Λ , so that the resulting measured wavefront will likely appear primarily as a streamwise tilt, similar to the wavefronts shown in Fig. 8. The mechanism by which the spark wavefronts appear primarily as a streamwise tilt is illustrated in Fig. 10; the effect that viewing aperture has on optical measurements is discussed in greater detail in [11].

Since the beacon wavefronts will appear primarily as a streamwise tilt, phase-lock averaging of the beacon measurements will be required to remove the effect of the spark tip/tilt noise; in this regard, the wind-tunnel feedforward AO approach is *more difficult* than for the operational system discussed above. Furthermore, since only a fraction of the shear-layer aberration will be captured by the beacon system, it will be difficult to determine the amplitude of the shear-layer aberration from the beacon measurements. This difficulty will be overcome by adjusting the phase of the beacon measurements with respect to the shear-layer forcing signal until the beacon wavefronts have the maximum slope; this slope will then be measured and used to compute the amplitude of the regularized shear-layer aberrations. In particular, the aberrations of the regularized shear layer are nearly sinusoidal in shape:

$$OPD \approx A \sin \frac{2\pi x}{\Lambda} \quad (4)$$

The amplitude A of the aberration described by Eq. (4) is related to the maximum slope as follows:

$$A = \frac{\Lambda}{2\pi} \left. \frac{dOPD}{dx} \right|_{\text{MAX}} \quad (5)$$

As pointed out above, the regularized shear-layer aberration is *not* a simple sinusoid, but can be accurately modeled by a combination of sinusoidal signals at the fundamental and first subharmonic of the forcing frequency; the exact relation for estimating the amplitude of the shear-layer aberration from the maximum slope will be determined prior to the feedforward AO tests. Once the phase and amplitude of the shear layer has been determined from the beacon wavefront measurements, the feedforward AO correction will be completed by adjusting the the DM to match this phase and amplitude. The success of the correction will be evaluated by measuring the residual aberration on a collimated scoring beam that passes through the shear layer and is reflected from the DM.

IV. Discussion

The results and discussion presented in this paper show that several benefits are realized by regularization of the shear layer as part of a feedforward AO approach prior to measurement using a laser-spark guide-star system. For example, as shown by Fig. 8, regularization of the shear layer allows removal of tip/tilt noise caused by spark jitter, by phase-lock averaging the beacon wavefronts using the shear-layer forcing signal; this kind of compensation for tip/tilt noise is essential for a system in which the beacon aperture is small compared to the aberration wavelength, but would likely not be necessary for a full-scale system. On the other hand, a full-scale system would still benefit from the fact that regularization of the shear layer shifts the frequency content of the shear-layer aberrations to a few discrete frequencies with large amplitude. Since the function of the beacon system in this case would be to simply measure the phase and amplitude of this large-amplitude regularized aberration, it is feasible that noise limits for the beacon system could be significantly relaxed, greatly simplifying the design of the system. Furthermore, as long as the beacon system can fulfill this function of accurately determining the phase and amplitude of the regularized aberrations, it would also likely not be necessary to compensate the beacon measurements for any anisoplanatic differences [1, 6] between the beacon and main beams. The performance requirements for a beacon system, when used in conjunction with a feedforward AO approach, will be reviewed in more detail in future investigations.

Acknowledgments

These efforts were sponsored by the Air Force Research Laboratory's Directed Energy Directorate, Kirtland Air Force Base, N.M., under Contract Number FA9451-08-C-0100. The U.S. Government is authorized to reproduce and distribute reprints for governmental purposes notwithstanding any copyright notation thereon.

References

- [1] Rennie, R. M., Whiteley, M. R., Cross, G., Cavalieri, D., and Jumper, E. J., "Measurement of Beacon Anisoplanatism Through a Two-Dimensional, Weakly-Compressible Shear Layer," AIAA Paper 2008-4215, June, 2008.
- [2] Rennie, R. M., Whiteley, M. R., Cross, G., Cavalieri, D., and Jumper, E. J., "Aero-Optic Measurements Using a Laser-Induced Air Breakdown Beacon," AIAA Paper 2009-4222, June, 2009
- [3] Tyson, R.K., *Principles of Adaptive Optics*, Academic Press, Inc., San Diego, 1991.
- [4] Rennie, R.M., Duffin, D.A., and Jumper, E. J., "Characterization and Aero-Optic Correction of a Forced Two-Dimensional, Weakly-Compressible Subsonic Free Shear Layer," *AIAA Journal*, November, 2008, pp.2787-2795.
- [5] Nightingale, A.M, Duffin, D.A., Lemmon, M., Goodwine, B., and Jumper, E.J., "Adaptive-Optic Correction of a Regularized Compressible Shear Layer," AIAA 2006-3072, June, 2006.
- [6] Whiteley, M.R., Welsh, B.M., and Roggemann, M.C., "Optimal modal wave-front compensation for anisoplanatism in adaptive optics," *J. Opt. Soc. Am. A*, **15**, no.8, Aug. 1998, pp 2097-2106.
- [7] Gordeyev, S., Post, M.L., McLaughlin, T., Ceniceros, J., and Jumper, E.J., "Survey of Optical Environment over Hemisphere-on-Cylinder Turret Using Suite of Wavefront Sensors," AIAA-2006-3074, June, 2006.
- [8] Gordeyev, S., Post, M.L., McLaughlin, T., Ceniceros, J., and Jumper, E.J., "Aero-Optical Environment Around a Conformal-Window Turret," *AIAA Journal*, Vol. 45, No. 7, 2007, pp.1514-1524.
- [9] Rennie, R. M., Siegenthaler, J. P., and Jumper, E. J., "Forcing of a Two-Dimensional, Weakly-Compressible Subsonic Free Shear Layer," AIAA 2006-0561, Jan., 2006.
- [10] Dimotakis, P.E., "Two-Dimensional Shear-Layer Entrainment," *AIAA Journal*, Vol. 24, No. 11, 1986, pp. 1791-1796.
- [11] Siegenthaler, J., Gordeyev, S., and Jumper, E. J., "Shear Layers and Aperture Effects for Aero Optics," AIAA-2005-4772, June, 2005.